Heat and Mass Transfer (2025) 61:12
https://doi.org/10.1007/s00231-024-03524-6

RESEARCH

Particle-resolved simulation of the pyrolysis process of a single plastic particle

Feichi Zhang[1] · Salar Tavakkol[1] · Flavio C. C. Galeazzo[2] · Dieter Stapf[1]

Received: 28 June 2024 / Accepted: 5 November 2024 / Published online: 9 December 2024

Abstract

Particle-resolved simulations have been performed to study the pyrolysis process of a high-density polyethylene (HDPE) particle in an inert hot nitrogen flow. The simulations resolve the velocity and temperature boundary layers around the particle, as well as the gradients of temperature and concentration within the particle. The objective of this work is to gain an in-depth understanding of the effect of particle morphology-specifically, the particle size and shape-on the interplay between heat transfer and pyrolysis progress, as well as to assess the applicable particle size when using the Lagrangian concept for simulating plastic pyrolysis. In all simulation cases, the pyrolysis reaction is initiated at the external surface of the particle, where the particle is heated the fastest. The reaction front propagates inward toward the core of the particle until it is fully pyrolyzed. For particle diameters larger than 4 mm, distinct temperature gradients within the particle can be detected, leading to a temperature difference of more than 10 K between the core and the external surface of the plastic particle. In this case, the Lagrangian simulations yield a considerably slower conversion compared with the particle-resolved simulations. Moreover, the cylindrical particle in longitudinal flow has been found to be pyrolyzed more slowly compared with the spherical and shell-shaped particles, which is attributed to the enhanced heat transfer conditions for the cylindrical particle. The results reveal the importance of considering particle morphology when modeling plastic pyrolysis. In addition, the Lagrangian approach, which assumes particle homogeneity, is only applicable for particle diameters smaller than 2 mm when modeling plastic pyrolysis.

1 Introduction

At present, only 9% of the worldwide 400 Mt plastic waste are recycled and 22% of them are mismanaged, for instance, disposed of in the nature or the oceans. The remaining 69% are either landfilled or incinerated, which negatively affects the environment and causes significant greenhouse gas emissions [1]. The main reason for the low recycling rate is that the conventional approach based on mechanical recycling can be used only for a subset of plastic products with high purity. In contrast, chemical recycling via pyrolysis is regarded as a promising technology that can be applied to recycle mixed and contaminated plastics. During the pyrolysis process, plastic polymers are thermally decomposed into their building blocks, which can be reused to produce new plastics. Pyrolysis generates a range of products, typically classified into three categories: volatile gases (including CO, CO_2, H_2, CH_4, and C_2-C_4 hydrocarbons), condensable vapors (comprising long-chain hydrocarbons and aromatic compounds) and solid residues (inorganic fractions and char) [2]. The key factors affecting pyrolysis product quality are the operating temperature, reactor types, feedstock composition, and catalysts [3].

The feasibility of pyrolysis technology for the chemical recycling of plastic waste has been verified in a large number of previous works, which were mostly performed on ideal, laboratory-scale reactors and focused on intrinsic degradation kinetics, product yields, reactor design, or the effect of catalysts [4–16]. However, the pyrolysis process in a real reactor system is accompanied by a number of complex thermo-physical phenomena such as hydrodynamics, heat transfer, and phase change, which interact with the pyrolysis reaction over a wide range of length and time scales. Despite the fact that the pyrolysis of biomass has been studied extensively in the past years, the results cannot be applied to plastic

✉ Feichi Zhang
feichi.zhang@kit.edu

[1] Institute for Technical Chemistry, Karlsruhe Institute of Technology, Karlsruhe, Germany

[2] High-Performance Computing Center Stuttgart, University of Stuttgart, Stuttgart, Germany

pyrolysis, as the thermo-physical properties of biomass and plastics differ significantly. In this case, a detailed understanding of the underlying thermo-fluid flow as well as its impact on the decomposition reaction of plastic polymers plays a vital role in up-scaling the pyrolysis process towards industrial applications. For instance, a fluidized bed reactor has major advantages in highly efficient, homogeneous heat transfer with fewer side reactions, which is regarded as a suitable reactor concept for the industrialization of the plastic pyrolysis process [17–22]. As the experimental study of the pyrolysis process is often limited by optical access due to the harsh environment in the reactors, numerical modeling represents an indispensable tool for designing the plastic pyrolysis process, as it takes the impact of real flow effects into account, provides a detailed insight into the underlying thermo-chemical mechanisms, and enables parameter studies at a large scale.

However, the modeling of plastic pyrolysis faces several challenges. First, in technical pyrolysis reactors like fluidized beds, the pyrolysis process is dominated by complex hydrodynamic flows, which include a large number of solid particles with different morphologies (shapes and sizes). In this case, modeling the underlying flow phenomena, such as gas-solid, solid-solid, and solid-wall interactions over different scales represents a difficult task [23, 24]. Moreover, the operational performance of plastic pyrolysis is severely limited by the heat transfer process when using large amounts of plastic mass. In particular, plastic melts and wets solid surfaces during the heating process, which can cause it to stick to other plastic particles or heat carrier materials [25]. Even the agglomeration of molten, sticky plastics with inert bed materials can lead to defluidization and clogging in fluidized bed reactors, causing serious operational problems [26]. In addition, the thermo-chemical decomposition of plastic polymers involves a large number of elementary reactions and chemical species, which are accompanied by phase transitions and chemical interactions during the pyrolysis of mixed plastics [27–30]. Therefore, there are currently no generally valid reaction mechanisms for the thermo-chemical degradation of plastic materials. Moreover, the mutual interactions between hydrodynamics, heat transfer, and chemical reactions prevail throughout the pyrolysis process, which occurs over a wide range of length scales. The hydrodynamic flow or gas residence time yields a time scale in the range of milliseconds to seconds, whereas the reaction time for the pyrolysis process can be as long as more than 30 minutes, leading to a disparity in the time scales for different processes.

According to these difficulties, modeling chemically-reacting, multiphase, multi-scale flows represents a significant challenge today. These are the main reasons why simulation studies considering real-flow effects on plastic pyrolysis can rarely be found currently. Previous simulation works on plastic pyrolysis have focused on applying available reaction kinetic models to predict product yields under varied operating conditions based on ideal, 0-dimensional (0D) setups, thus neglecting the effects of flow and heat transfer [31]. Zhang et al. [32] proposed a 0D single-particle model, where the heating of plastic particles via convective heat transfer has been considered. In [33], 3-dimensional (3D) Eulerian-Eulerian simulations were performed to study the pyrolysis process of biomass and plastic mixtures in a fluidized bed reactor, which resolves the multiphase reactive flow with a multi-component, multi-step reaction mechanism for the pyrolysis reaction. More recently, the pyrolysis of waste plastics in a rotary furnace has been studied using the hybrid computational fluid dynamics and discrete element model (CFD-DEM) approach by Zhang et al. [34]. Currently, CFD-DEM represents one of the most advanced approaches in modeling plastic pyrolysis, as it combines the fluid dynamics of the gas phase with particle dynamics to simulate the behavior of plastic particles in a pyrolysis reactor [35]. As DEM-type simulations are computationally extremely expensive, general Lagrangian models coupled with sophisticated particle-collision models, such as the multiphase particle-in-cell (MP-PIC) approach, can be applied for simulating plastic pyrolysis in technical reactor systems [23]. However, challenges remain in accurately modeling the melting behavior of plastics and incorporating particle non-sphericity and polydispersity.

In large-scale pyrolysis plants, the efficient heating of plastic polymers and control of reactor temperature are essential to ensure product quality. In particular, plastic materials generally have high thermal resistance, so heat transfer may represent a limiting process compared to the pyrolysis reaction. Moreover, plastic wastes are shredded before being fed into the reactor, leading to broad distributions in the size and shape of plastic particles. In an attempt to gain a detailed understanding of the thermo-chemical conversion process during plastic pyrolysis, highly resolved numerical simulations have been carried out to study the effect of particle shape and size on the pyrolysis process of a single plastic particle. The boundary layers and the internal gradients of the particle have been resolved on the computational grid in order to study the detailed heat transfer process caused by different particle shapes, as well as its mutual interplay with the pyrolysis reaction. Another objective of this work is to scrutinize the application range of the commonly used Lagrangian approach in terms of applicable particle size. This work reveals for the first time the effect of particle morphology on the plastic pyrolysis process through fully 3D, particle-resolved simulations, along with an assessment of applicable particle size using the Lagrangian method.

2 Modeling of multiphase reactive flow

An Eulerian-Eulerian approach has been applied to simulate the gas-solid flow with the pyrolysis of a single plastic particle. In this method, two sets of balance equations in the Eulerian framework are solved, representing the gaseous and solid phases, which are coupled through source terms that consider mass, heat, and momentum exchange. The gas-solid phases are identified by means of the void fraction ε, which is 1 for the pure gas phase and 0 for the pure solid phase. The shape of the particle is considered by setting the initial field of ε to 0 for the zones where the particle is placed. As the particle is heated over time, the pyrolysis process is initiated by the local particle temperature via an Arrhenius-type rate law. The pyrolysis conversion leads to mass transfer from solid to gas, which is controlled by the reaction source terms in the mass balance equations. The void fraction increases during the pyrolysis process due to mass transfer from solid to gas phase, leading to the shrinkage of the particle and variation of the local heat transfer coefficient at the deformed interface. In the following, the balance equations solved for species mass, total mass, energy, and momentum for both gas and solid phases are presented.

2.1 Conservation of species mass

The species mass conservation equation of the gas phase is given by

$$\frac{\partial}{\partial t}\left(\varepsilon\rho^f\langle Y_i\rangle^f\right)+\nabla\cdot\left(\rho^f\langle Y_i\rangle^f\langle\mathbf{u}\rangle\right)-\nabla\cdot\left(\varepsilon\rho^f D_{\text{eff}}\nabla\langle Y_i\rangle^f\right) = \varepsilon\langle\dot{\omega}\rangle^f+(1-\varepsilon)\langle R_i\rangle^s \tag{1}$$

where $\langle\cdot\rangle$ indicates spatially filtered values and $\langle\cdot\rangle^f$ represents values from the fluid (gas) phase. The fluid velocity is given by $\mathbf{u}$; Y_i denotes the mass fraction of the i-th species; ρ is the fluid density and $\dot{\omega}$ indicates the reaction rate of the i-th species resulting in the gas phase. The term D_{eff} represents the effective diffusion coefficient, which takes into account the effects of local structures in the porous media and the grid size. The term $\langle R_i\rangle^s$ is the source term caused by volatile species released from the solid particle due to the pyrolysis reaction. Analogously, for the solid phase, the species mass conservation equation is given by

$$\frac{\partial}{\partial t}\left((1-\varepsilon)\rho^s\langle Y_k\rangle^s\right)=(1-\varepsilon)\langle R_k\rangle^s \tag{2}$$

where $\langle\cdot\rangle^s$ denotes values derived from the solid phase. The mass fraction of the k-th solid species is Y_k and R_k is the reaction source term caused by the heterogeneous pyrolysis reaction. The density of the gas is calculated using the equation of state for nitrogen as an ideal gas. High-density polyethylene (HDPE) is used in this work as feedstock, which has a density of $\rho_P = 950$ kg/m^3.

2.2 Conservation of total mass

The continuity equation for the gas phase yields

$$\frac{\partial}{\partial t}\varepsilon\rho^f+\nabla\cdot(\rho^f\mathbf{u})=(1-\varepsilon)\sum_i\langle R_i\rangle^s \tag{3}$$

where the source term on the right-hand side (r.h.s.) takes into account the mass released from the solid particle by the pyrolysis reaction. Similarly, the mass balance equation for the solid phase yields

$$\frac{\partial}{\partial t}(1-\varepsilon)\rho^s=(1-\varepsilon)\sum_k\langle R_k\rangle^s \tag{4}$$

with the source term $\langle R_k\rangle^s$ considering the mass loss of solid particle due to the pyrolysis reaction. At present, there are no detailed kinetic models available for plastic pyrolysis that can be applied to CFD simulations. Some lumped kinetic models exist, where product groups have been classified according to the number of C-atoms or boiling points; however, these are only valid under the specific conditions used in the experiments. As the focus of the current work is to reveal the importance of particle morphology on the overall conversion, a one-step kinetic mechanism has been used for modeling the pyrolysis reaction (plastic→product). An Arrhenius-type rate law is commonly used to describe the degradation reaction for plastic pyrolysis [31], where the reaction rate is evaluated with

$$R_k=k_r\rho^s\langle Y_k^s\rangle,\quad k_r=k_0\exp\left(-\frac{E_a}{RT_p}\right) \tag{5}$$

The pre-exponential factor k_0 and activation energy E_a are set as $k_0 = 4.22\times10^{22}$ s^{-1} and $E_a = 346.8$ kJ/mol according to [36] for the pyrolysis of HDPE. The reaction enthalpy has been estimated to be 5% of the lower heating value of HDPE [37], which is comparable with the measured heat of reaction proposed in [38].

2.3 Conservation of energy

For the gas phase, the enthalpy conservation equation is given by

$$\frac{\partial}{\partial t}\varepsilon\rho^f c_p^f\langle T\rangle^f+\nabla\cdot(\rho^f c_p^f\langle T\rangle^f\langle\mathbf{u}\rangle)=\nabla\cdot\nabla(\varepsilon k_{\text{eff}}^f\langle T\rangle^f)-\varepsilon\sum_i h_{f0,i}\langle\dot{\omega}_i\rangle^f -\langle q_{\text{conv}}\rangle+(1-\varepsilon)\langle T\rangle^f\sum_i c_{p,i}\langle R_i\rangle^s+\langle S^{\text{f,rad}}\rangle \tag{6}$$

T represents the gaseous temperature and the specific heat under constant pressure for the fluid is denoted as c_p; k_{eff}^f

stands for the effective thermal conductivity of the fluid. The sum of the products of the reaction rate $\dot{\omega}_i$ with the specific enthalpy $h_{0,i}$ denotes the heat release rate due to the gas phase reaction. The thermal conductivity and heat capacity of nitrogen are evaluated as functions of the gas temperature. The effective heat flux transferred from the gas to the solid phase $\langle q_{\text{conv}} \rangle$ is calculated with

$$\langle q_{\text{conv}} \rangle = \alpha \Sigma (\langle T \rangle^f - \langle T \rangle^s) \tag{7}$$

α is the convective heat transfer coefficient, which is evaluated in terms of the Nusselt number Nu

$$\alpha = \frac{Nu \cdot \lambda_f}{L_C} \tag{8}$$

where λ_f is the fluid thermal conductivity and L_C is the characteristic length. Nu has been calculated using empirical correlations which depend on geometry of the feedstock and flow condition [39]. Σ in Eq. 7 is the volume-specific surface area, which is estimated to be $\frac{1}{2\Delta}$, with Δ being the grid resolution. S^{rad} in Eq. 6 accounts for heat exchange through radiation, which is neglected in this work.

For the solid phase, the equation of energy yields

$$\begin{aligned} \frac{\partial}{\partial t} \rho^s c_p^s \langle T \rangle^s (1-\varepsilon) = \nabla \cdot ((1-\varepsilon) \mathbf{K} k_{\text{eff}}^s \cdot \nabla \langle T \rangle^s) - (1-\varepsilon) \sum_k h_{f,k}^0 \langle R_k \rangle^s \\ + \langle q_{\text{conv}} \rangle - (1-\varepsilon) \langle T \rangle^f \sum_i c_{p,i} \langle R_i \rangle^s + \langle S^{\text{f,rad}} \rangle \end{aligned} \tag{9}$$

where c_p^s is the specific heat capacity of solid and k_{eff}^s denotes the effective conductivity, which is calculated as the mass fraction average of the heat conductivity of the individual solid phase components. As the solid phase has only one component in the current work, k_{eff} corresponds to the heat conductivity of HDPE with $\lambda_P = 0.4$ W/m/K. The heat capacity of HDPE is set to $c_{p,P} = 2133$ J/kg/K. The anisotropy tensor $\mathbf{K}$ of the solid matrix accounts for the non-isotropic effect of heat condition in the porous media consisting of solid and gas phase. The plastic material itself is homogeneous and yields an isotropic heat conductivity. The heat transfer due to thermal radiation has been neglected due to the relatively low reactor temperature ($T_R < 500$°C).

2.4 Conservation of momentum

The solid particle is immobilized and; therefore, no momentum equation is solved for the solid phase. The momentum conservation for the gas phase is given by

$$\begin{aligned} \frac{\partial}{\partial t} \rho^f \langle \mathbf{u} \rangle + \nabla \cdot (\rho^f \langle \mathbf{u} \rangle \langle \mathbf{u} \rangle) = -\varepsilon \nabla \langle p \rangle^f + \nabla \cdot (\mu_{\text{eff}} \nabla \langle \mathbf{u} \rangle) \\ + \rho^f \mathbf{g} - \mu_{\text{eff}} \mathbf{D} \cdot \langle \mathbf{u} \rangle - \mathbf{F} \cdot \langle \mathbf{u} \rangle \end{aligned} \tag{10}$$

where μ_{eff} is the dynamic viscosity and $\mathbf{g}$ the gravitational acceleration. $\mathbf{D}$ denotes the Darcy coefficient, which models the loss of momentum of the gas phase within the solid phase. The Forchheimer coefficient $\mathbf{F}$ is similar to the Darcy coefficient and accounts for the effects of turbulent flow. Due to the laminar flow conditions used in the current study, this coefficient is set to zero.

In summary, two sets of balance equations are solved for the solid and gas phases on the same computational grid in the current method, where the different phases are identified by means of the void fraction. The balance equations for the gas and liquid phases are coupled through source terms concerning mass and heat exchange. The model resolves the boundary layers and the particle-internal gradients, so that it is suitable for studying the effects of particle size and shape on the heating and pyrolysis processes, as well as their mutual interactions. In technical pyrolysis plants, however, plastic melts before initiation of the chemical decomposition, where pyrolysis vapors may leave the molten plastic droplets as small bubbles. The melting of plastic represents one of the general challenges in modeling pyrolysis of plastics. This issue is not considered in the current work, as no sub-model is available for the description of the complex rheological, morphological behavior of molten plastics at this time. Further limitations include immobilization of the solid phase and use of a simplified one-step pyrolysis reaction. Despite these processes are not considered, good agreements between calculated and measured results have been achieved by using 0D kinetic models for the TG setup in [31, 32]. Therefore, it is argued that the effect of melting on the overall pyrolysis progress is subordinate for single, relatively small particles.

The solver "porousGasificationFoam" developed in the open-source code OpenFOAM by Zuk et al. [40] has been used for the simulations, where the proposed Eulerian-Eulerian approach for modeling multiphase reactive flow is implemented. The governing equations are solved using a fully implicit scheme of second-order accuracy for the time integration (backward) and a second order interpolation scheme for discretizing the convective term. All diffusive terms are discretized with a bounded scheme of second order accuracy, as well. The pressure-implicit split-operator (PISO) algorithm is employed for pressure correction. A detailed description of7 the simulation method can be found in [40].

3 Simulation setups

3.1 Operating conditions

In technical pyrolysis plant like fluidized bed or screw reactors, the plastic particles are subjected to complex flow field to enhance the rate of heat transfer. This work aims to reveal

the effect of different heating conditions on the pyrolysis conversion of a single plastic particle by varying the particle size and shape, which serves as a fundamental study towards more realistic conditions. For that reason, spherical plastic particles with different diameters of $d_P = 1.8$, 2.7, 4 and 6 mm were used as feedstock in order to study the effect of particle size on the pyrolysis process. In addition, particles with a constant mass of 10 mg were simulated in spherical, cylindrical and shell shape, in order to study the influence of particle shape on the pyrolysis process. The cylindrical particle has an aspect ratio of unity, which is defined as the ratio of cylinder height to its diameter. These morphological parameters of the particle result in modified heating conditions of the plastic particle and different scenarios for the interplay between heat transfer and pyrolysis reaction. Table 1 summarizes the simulation conditions, along with the dimensionless Reynolds number Re and Biot number Bi

$$Re = \frac{v_G \cdot L_C}{\nu_G}, \quad Bi = \frac{L_C/\lambda_P}{1/\alpha} = \frac{\alpha \cdot d_P}{\lambda_P} \tag{11}$$

Bi represents the ratio of the conductive heat resistance within the solid body to the convective heat resistance outside the body. For all cases, Bi is smaller than unity, indicating that the heating process is limited by the convective heat transfer.

In practice, municipal plastic wastes are shredded before feeding into the pyrolysis reactor, which leads to a broad distribution of particle size and shape for the plastic feedstock. As the particle-resolved simulation is computationally expensive due to resolution of the mm-sized particle on the grid and running the simulation for a physical time of more than 30 min, only the most fundamental geometries along with a few variations on particle size have been used to reveal the importance of particle morphology for modeling plastic pyrolysis. Considering plastic pyrolysis in technical reactor system like fluidized bed, where the plastic particles are mixed with hot energy carriers like sand, the shell-shaped particle is designed specifically to mimic the sticking of molten plastic around an inert solid particle like sand. For comparison reason, the size and mass of the shell are set similar to those of the spherical and cylindrical particle, using an internal and an external diameter of 2 mm and 3 mm.

Table 1 Operating parameters used for simulation of plastic pyrolysis of a single particle in a hot nitrogen flow at a temperature of 500°C

Shape	Diameter [mm]	Mass [mg]	Re [-]	Bi [-]
Sphere	1.82	3	0.56	0.31
	2.7	10	0.84	0.33
	4.0	32	1.24	0.34
	6.0	107	1.85	0.36
Cylinder	2.4	10	0.74	0.11
Shell	3.0	10	0.93	0.33

3.2 Computational domain

A cylindrical computational domain is used for the simulation, whose diameter and length increase with the used particle size. The temperature at all boundaries is fixed to the desired reactor temperature. The circumferential and upper surfaces of the cylinder are defined as opening, where the velocity boundary condition is set as zero-gradient. The lower surface of the cylinder is used as inlet, where hot nitrogen gas enters the domain. The plastic particle is placed at the center of the cylinder, as shown in Fig. 1(a). The diameter and length of the cylindrical domain are 5.3 mm and 15 mm for the particles with diameters smaller than 3 mm. For the larger particles with diameters of 4 mm and 6 mm, the diameters of the domain have been enlarged to 10.6 mm and 21.2 mm, along with corresponding lengths of 30 mm and 60 mm. Figure 1(b-d) depict a side view, the mesh topology on a meridian cutting plane passing through the centerline axis and a cross-sectional view of the computational grid. An equidistant grid resolution of 0.35 mm has been used for all cases, which was selected according to a grid-independent study (see Fig. 5) and a compromise between computational effort and accuracy. For numerical stability reason, the time step for the simulations have been set to 1 ms, which ensures the Courant-Friedrichs-Lewy (CFL) number smaller than unity.

3.3 Verification of the numerical model

Simulations have first been performed for the thermogravimetric (TG) experiments made by Ceamanos et al. [36], where the plastic particle is heated at a given heating rate. This case is used to verify the overall capability of the model for the simulation of plastic pyrolysis process. Compared with the commonly used 0D models for validation of chemical kinetic parameters, the current approach resolves the particle-internal fields and boundary layers around the particle for a 3D, multiphase, reactive flow. In the following section, simulations at constant reactor temperatures or under isothermal conditions have been conducted to study the effects of particle size and shape on the pyrolysis process. For modeling of the TG experiments, both the experimental data and simulation parameters were sourced from Ceamanos et al. [36] for the pyrolysis of HDPE samples. In the experiment, the plastic particle is hold in a crucible, whose temperature is measured. As the plastic particle melts, it wets on the crucible. Therefore, temperature of the plastic sample is commonly assumed to be equal to temperature of the crucible. A constant heating rate of $\beta = 12°$ C/min was used at the starting temperature of 27°C, whereas the final temperature was T_R = 450°C and 470°C.

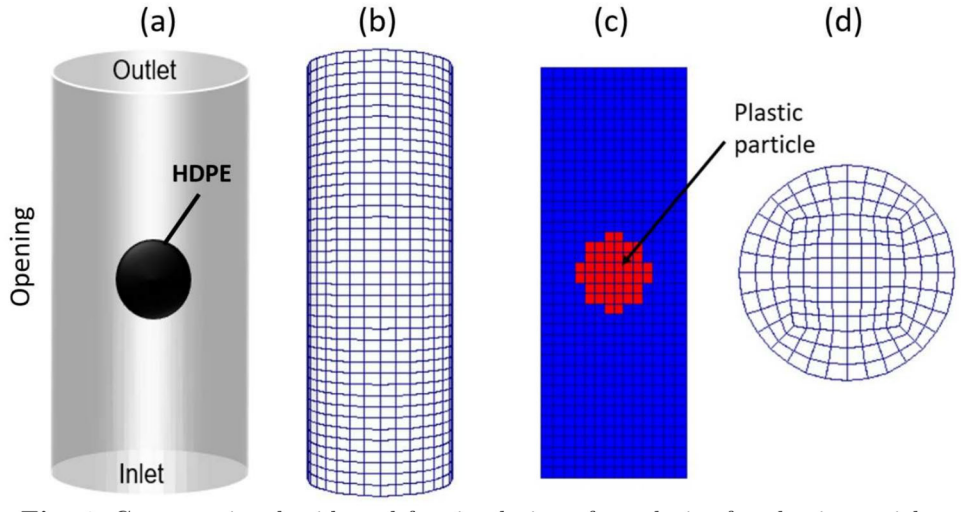

Fig. 1 Computational grid used for simulation of pyrolysis of a plastic particle

This time-varying temperature profile has been used for all boundaries of the computational domain. The initial mass of the feedstock is $m_0 = 3$ mg, corresponding to a diameter of $d_P = 1.82$ mm of a spherical particle. The inlet gas velocity is set to 2.5 cm/s according to the volume flow rate used in the TG experiment, which ensures a laminar flow regime. This velocity is adopted for the subsequent studies at isothermal conditions. Figure 2 compares the conversion progress obtained from the simulations and experiments, which is defined as

$$X = \frac{m_0 - m_P}{m_0} \tag{12}$$

with m_P and m_0 being the current and start mass of the plastic particle. The mass of plastic particle is calculated by volume integration of the solid volume fraction over the whole computational domain, which is multiplied with the density of the particle. In all cases, X increases from $X = 0$ (unpyrolized state) to $X = 1$ (fully pyrolized state).

As shown in Fig. 2, the calculated and measured X agree well with each other. The conversion process starts after 30 min, which is due to heating of the particle from the initial temperature at 27°C to a temperature of higher than 400°C, at which the pyrolysis reaction takes place. The deviations between the calculated and measured X may be attributed to the assumptions used in the simulation. For instance, the feedstock is placed on a crucible base in the experiment, whereas it is subjected to a hot gas flow in the simulations. In addition, the current simulations have not considered the melting process of the plastic and only a single-step chemistry has been used in this work. Despite these differences, the simulations have reproduced the experimental results with a reasonably good accuracy, which justifies the proposed numerical model.

In the current case, the reactor temperature is heated at a heating rate of 12°C/min, which is selected according to the dynamic TG experiments in [36]. In technical pyrolysis plants, plastic is fed into a pre-heated, isothermal reactor, where the particle is heated faster. However, once the pyrolysis process starts, the particle temperature increases only slightly due to the endothermic pyrolysis reaction and the small temperature difference between the gas/solid phases, that drives the heating process (see also Fig. 3a). The same behavior has been confirmed in [32], where simulations of plastic pyrolysis applying reaction kinetic coefficients obtained from TG experiments revealed only a slight increase of particle temperature after onset of the pyrolysis reaction under isothermal conditions. Therefore, the kinetic parame-

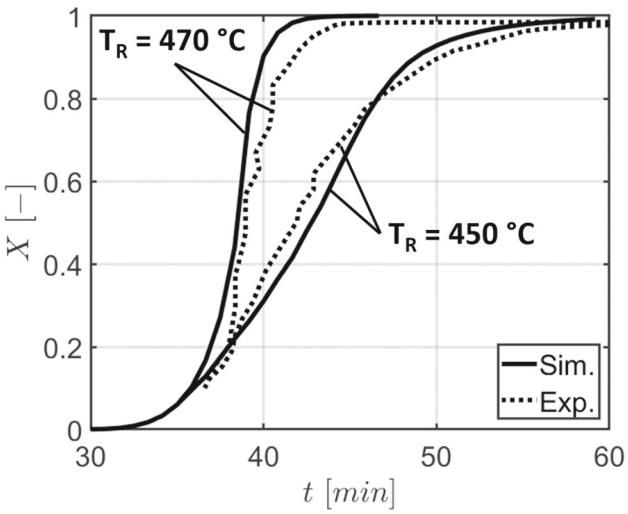

Fig. 2 Comparison of calculated and measured conversion progresses for the operating parameters used by the TG experiment in [36]

ters derived from TG experiments at relatively low heating rate could be used for modeling the pyrolysis reaction .

4 Results

In this section, the pyrolysis process of single HDPE particles in a hot, isothermal nitrogen flow are simulated. A parametric study was carried out with regard to the effects of particle shape and size on the pyrolysis process. Furthermore, a comparison of the particle-resolved simulation with the commonly applied Lagrangian method has been conducted to scrutinize the application range of the Lagrangian assumptions with regard to the use of ideal, homogeneous particles for modeling plastic pyrolysis in the current single-particle setup.

4.1 Effect of particle morphology

In the previous case using the TG experiment, the temperature of the reactor wall was prescribed by the given heating rate. In the following, all boundaries of the cylindrical domain have been fixed at the reactor temperature with $T_R = 470°C$. Figure 3 shows the time evolution of particle temperature T_P at the center of the spherical particles Fig. 3(a) and of the conversion progress Fig. 3(b) by using different diameters, i.e., d_P = 1.8, 2.7, 4 and 6 mm. The particle temperature increased drastically to a value of above 400°C due to convective heat transfer. Thereafter, it increased slowly until it reached the reactor temperature. This can be explained by the fact that the pyroylsis process is an endothermic reaction, which counteracts the heating process. In particular, the small temperature difference between the particle and the surroundings during the conversion stage leads to a weakened heating rate. When the reaction rate is high, the introduced heat from the gas is balanced out by the endothermic reaction, so that the particle temperature increases only slowly after onset of the pyrolysis reaction. As the pyrolysis reaction approached its final stage, the reaction rate or the effect of endothermic reaction was subordinate, at the same time, the heat transfer was enhanced due to the decreased size of the particle. As a result, the heating of particle dominated the heat loss caused by endothermic reaction, leading to an increase of particle temperature, until it reached the gas temperature at the end. In this way, the competing interaction between the heat transfer and the endothermic pyrolysis reaction controls the particle temperature and the pyrolysis progress. The smaller particle was heated up faster than the larger particle and the pyrolysis reaction took place at a higher temperature for the smaller particles, which can be detected by the temperature profiles shown in Fig. 3.

Figure 4 shows the calculated conversion progresses from the simulations using different particle shapes and flow directions (see Table 1), where all particles have a constant mass of 10 mg. The cylindrical particles have an aspect ratio of unity, which are placed perpendicular and parallel to the main flow. The pyrolysis of the shell particles was slightly slower compared with the spherical particle, because the shell particle was slightly larger than the spherical particle, leading to a lower heating rate of the particle. In contrast, pyrolysis of the cylindrical particles was considerably slower than that of the spherical and shell particles, which was attributed to the lower heat transfer coefficient for the cylindrical particles. In addition, the cylindrical particle in cross-flow is pyrolized faster than that in longitudinal flow, which is caused by an enhanced heat transfer efficiency in case of fluid flow perpendicular to the axis of the cylinder. In contrast, longitudinal flow, where the fluid flow is parallel to the cylinder's axis, tends to have a more stable boundary layer, resulting in lower heat transfer rate. The results reveal the importance of particle shape and flow direction on the pyrolysis process.

In order to validate the grid resolution used in this work, a grid-independent study has been performed applying twice-refined grids with a resolution of 0.17 mm for the d_P = 2.7 mm and 4 mm spherical particles. As shown in Fig. 5, the calculated conversion progress obtained from simulations

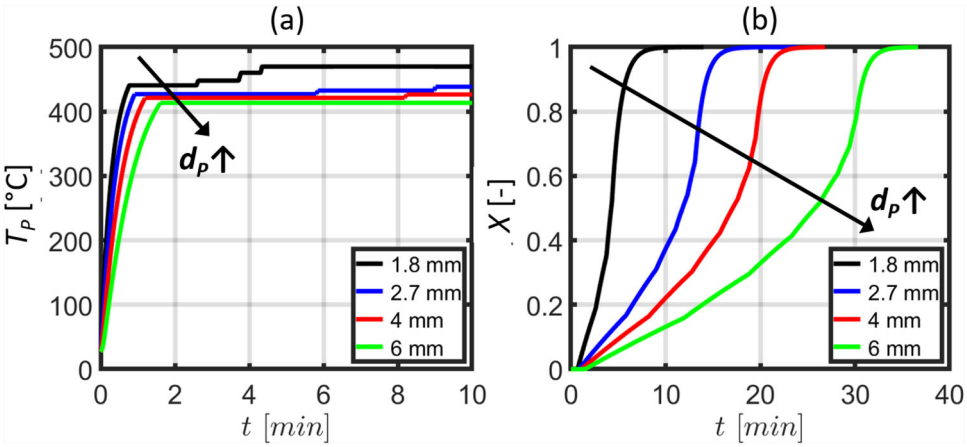

Fig. 3 Time evolution of particle temperature (a) and conversion progress (b) calculated from particle-resolved simulations using different sizes of plastic particle

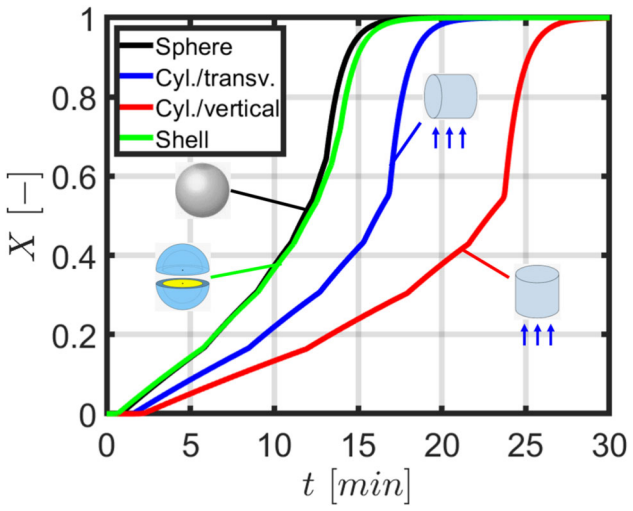

Fig. 4 Comparison of calculated pyrolysis progresses from particle-resolved simulations for a HDPE particle with different shapes

using both reference and refined grids agree well with each other, which validates the grid resolution with 0.35 mm used in the current study.

4.2 Particle-resolved vs. Lagrangian method

As the particle-resolved simulation is computationally expensive due to resolution of the particle-internal gradients and boundary layers, the Eulerian-Lagrangian method is commonly applied for modeling multiphase, reactive flows with a large number of solid particles. In this method, Lagrangian particles are introduced into the computational domain, whose trajectories are tracked over time. These Lagrangian

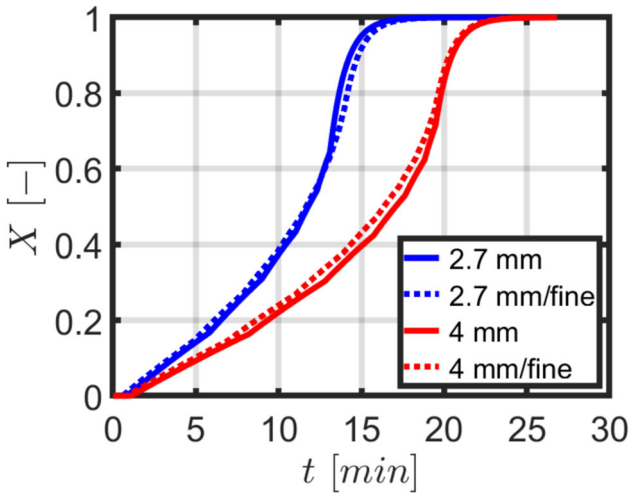

Fig. 5 Comparison of calculated time evolution of pyrolysis progress by using different grid resolutions of 0.35 mm and 0.17 mm

particles interact with the continuous gas flow, where both phases are coupled through source terms concerning mass, momentum and heat transfer.

In general, the Lagrangian method assumes ideal, homogeneous particles with constant properties within the whole particle volume. In addition, the flow and thermal boundary layers are not resolved due to the use of considerably larger cell volumes than the particle size. In this way, the Lagrangian method can be applied to systems having a large number of particles. In order to assess the capability of the Lagrangian method for modeling plastic pyrolysis, it has been applied to simulate plastic pyrolysis with the same operating conditions as used for the particle-resolved simulations.

Figure 6 shows instantaneous contours of the particle temperature T_S and the streamswise flow velocity U_Z on a meridian cutting plane passing through the symmetry axis for the cases with $d_P = 4$ and 6 mm. The velocity vectors (black arrows) indicate flow directions and magnitude of the flow velocity. The temperature gradient within the particle can be clearly detected for these cases. The differences between the surface and core temperature is as large as 6 K for the 4 mm particle and 10 K for the 6 mm particle, which are not resolved by the Lagrangian approach. Moreover, the flow velocity in the gas phase decreased to 0 at the surface of the particle due to the non-slip condition, leading to a stagnation zone in front of the particle and a wake region behind it with low flow velocity. The results reveal that the velocity and thermal boundary layers are not uniformly distributed along the particle surface, or the particle is not heated up uniformly, indicating uncertainties of the Lagrangian method.

Figure 7 compares time evolution of the particle temperature at the center of the particle (Fig. 7a) and the conversion progress (Fig. 7b) calculated with the particle-resolved (solid lines) and Lagrangian method (dotted lines). Generally, we observe that the results from both particle-resolved and Lagrangian methods exhibited similar behaviors in terms of qualitative effect of the particle size on the heating and conversion progress. However, the particles are heated more slowly in the Lagrangian compared with the particle-resolved simulations. This is attributed to the fact that the particle is heated up in whole in the Lagrangian method due to the assumption of homogeneity. On the contrary, the resolved particle is heated up gradually from its surface to the core region. For the case with $d_P = 1.8$ mm, the particle temperature calculated from both methods agree well with each other, indicating that the Lagrangian method is applicable for this case with small diameter. With increasing size of the particle, the heat conduction within the particle becomes increasingly important, leading to large deviations between calculated particle temperatures from both methods.

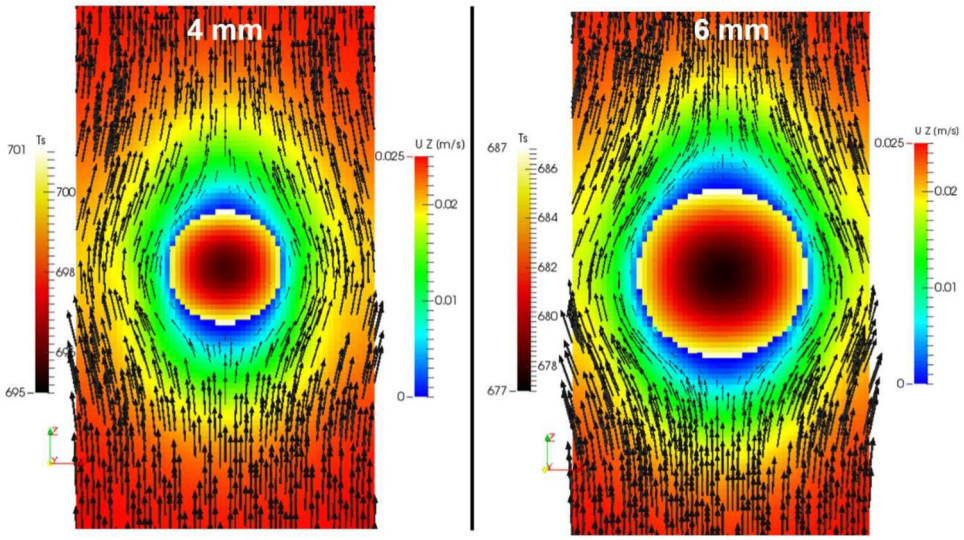

Fig. 6 Contours of instantaneous particle temperature T_S and flow velocity in streamswise direction U_Z for two particle sizes with diameters at 4 mm and 6 mm

The same behavior can be detected for the reaction progress shown in Fig. 7b, where the slower heating rate in the Lagrangian model has led to a delayed pyrolysis conversion compared with the particle-resolved model. For the particle with $d_P = 1.8$ mm, the agreement between calculated conversion progress from both methods is good. However, for the case with $d_P = 6$ mm, the reaction started after 10 minutes in the Lagrangian simulation, whereas the conversion had started much earlier in the particle-resolved simulation. This is because a longer time is needed to reach a homogeneous temperature for the whole particle in the Lagrangian model, at which the pyrolysis reaction can proceed. On the contrary, the particle is heated first at its surface in the particle-resolved simulation, so that the onset of the pyrolysis reaction is earlier in this case. The differences between particle temperature in the core and the external surface is negligible for small particles, which increases with the size of particle, as depicted in Fig. 6 for the particles with $d_P = 4$ mm and $d_P = 6$ mm. Therefore, the calculated conversion progresses by using both methods differ significantly for large particles. The results reveal that the Lagrangian method is applicable only for particles with a size of smaller than 2 mm.

4.3 Effect of reactor temperature

The reactor temperature T_R represents one of the most important operating parameters for plastic pyrolysis, which influences the reaction rate and the product yield. In case of

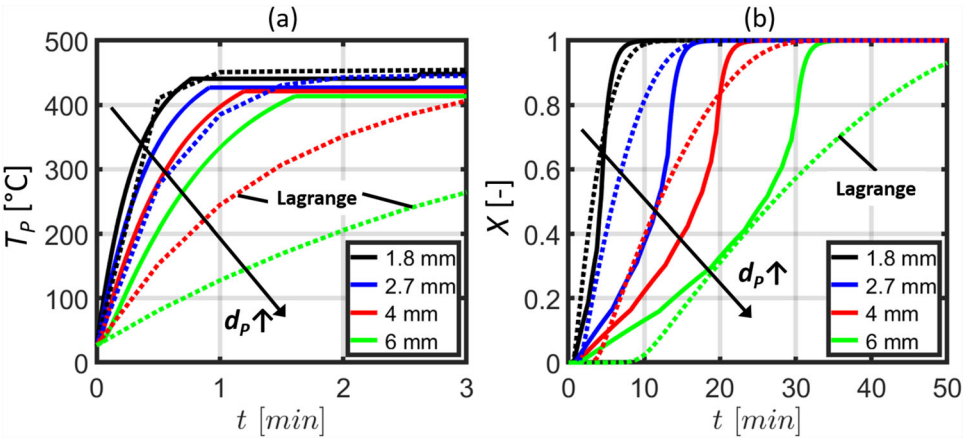

Fig. 7 Comparison of calculated particle temperature (a) and reaction progress (b) from particle-resolved (solid lines) and Lagrangian simulations (dotted lines) for different particle sizes

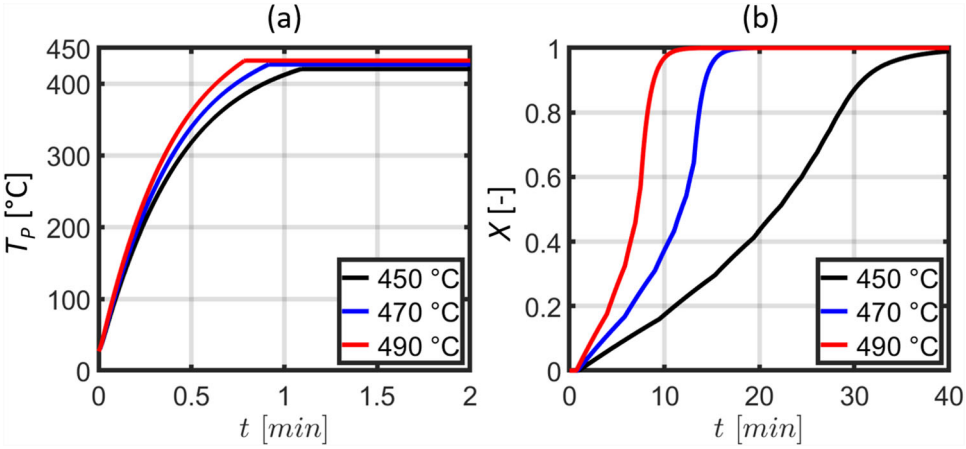

Fig. 8 Effect of reactor temperature on the particle temperature (a) and the conversion progress (b) during pyrolysis of a HDPE plastic particle

increased reactor temperature, the heat transfer is enhanced due to the large temperature difference between the solid and the gas phase. In addition, the pyrolysis reaction takes place at higher temperature, leading to a larger reaction rate. Figure 8 compares the calculated time evolution of the particle temperature at the kernel (Fig. 8a) and the conversion progress (Fig. 8b) for the spherical particle with a mass of 10 mg at different reactor temperature T_R ranging from 450°C to 490°C. It is evident that the particle is heated and pyrolized faster at elevated T_R. Furthermore, the pyrolysis temperature, which was determined by the balance of gas-to-solid heat transfer and the endothermic reaction, increased with T_R, which can be identified by the quasi steady-state range of T_P in Fig. 8a for $t > 1$ min.

4.4 Heat transfer vs. pyrolysis reaction

To assess the interplay between the heat transfer and the pyrolysis reaction, the pyrolysis number Py is introduced, which is defined as the ratio of the characteristic time scales of the chemical reaction τ_c to that of the convective heat transfer τ_h [41]

$$Py = \frac{\text{Time scale of chemical reaction}}{\text{Time scale of heat transfer}} = \frac{\tau_c}{\tau_h} = \frac{1/k_r}{\rho_P c_{p,P} d_P/\alpha} = \frac{\alpha}{k_r \rho_P c_{p,P} d_P} \tag{13}$$

where α is the heat transfer coefficient and k_r is the rate constant provided at the given reactor temperature; ρ_P and $c_{p,P}$ are the density and the specific heat capacity of the particle. When the chemical reaction is slower than the heat transfer process ($Py > 1$ or $\tau_c > \tau_h$), the pyrolysis process is limited by the pyrolysis reaction. In contrast, the whole conversion process is limited by the heat transfer when the heating process is slower than the pyrolysis reaction, i.e., $Py < 1$ or $\tau_c < \tau_h$.

Figure 9 depicts the calculated pyrolysis time t_{py} against Py for the cases with spherical particles, where t_{py} is defined for the time duration from $X = 1\%$ to $X = 99\%$. The reactor temperature T_R was kept constant at 470°C while varying the particle size (black line) and the particle size was kept constant at $d_P = 2.7$ mm ($m_P = 10$ mg) while varying T_R (red line). The parameters used in Eq. 13 are evaluated for the given reactor temperatures. The heat transfer coefficient α is calculated from the Nusselt correlation, as shown in Eq. 8; the rate coefficient k_r is obtained from the Arrhenius-type law shown in Eq. 5. The heat capacity of HDPE is set to 3800 J/kg/K [38], along with a density of 950 kg/m^3.

As depicted in Fig. 9, Py is smaller than unity for the most cases, indicating that the heat transfer process is slower compared with the pyrolysis reaction ($\tau_h > \tau_c$). In this case,

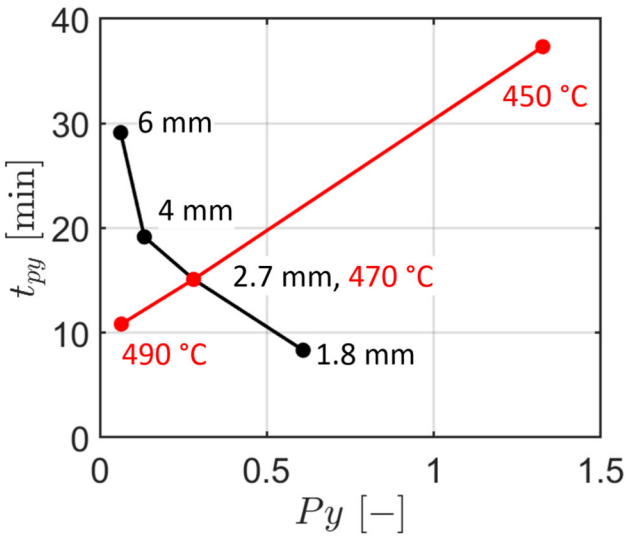

Fig. 9 Correlation of pyrolysis time with pyrolysis number

an enhanced heating of the particle can effectively accelerate the pyrolysis process. The reaction time scale τ_c decreased with T_R due to increase of the reaction rate, which leads to a decrease of Py. As the conversion time t_{py} decreases with T_R, t_{py} yields a positive correlation with Py while varying T_R, as shown in Fig. 9. Py is larger than unity or the reaction is slower compared with the heating process for the case with $T_R = 450°C$, indicating that the pyrolysis reaction represents the limiting process for the overall conversion. Based on the results shown in Fig. 9, the required residence time of plastic materials can be predicted in terms of Py at given operating conditions. The challenge in this case is to assess the heating condition for the specific reactor systems.

5 Conclusion

Numerical simulations have been performed to study the pyrolysis process of a high-density polyethylene (HDPE) particle in a hot nitrogen flow, which resolve the particle-internal gradients of temperature and concentration as well as the boundary layers around the particle. The objective of the work was to reveal the impact of particle shape and size on the interplay between the heating and pyrolysis processes, as well as to assess the applicable particle size while using Lagrangian method for the simulation of plastic pyrolysis. The main findings are summarized below:

- The cylindrical particle in longitudinal flow is pyrolyzed at slowest compared to the spherical and shell-shaped particles at the same mass and reactor temperature.
- For spherical plastic particles with a diameter of $d_P >$ 2 mm, distinct temperature gradients within the particle can be observed, with a maximum temperature difference of more than 10 K for the largest particle with $d_P = 6$ mm.
- The Lagrangian and particle-resolved simulations showed good agreement for particles with diameters smaller than 2 mm. However, the discrepancies between the two methods increase significantly with the particle size.
- The pyrolysis time exhibits a strong correlation with the pyrolysis number, which is defined as the ratio of characteristic timescale of the pyrolysis reaction to that of heat transfer.

The results reveal the significant impact of particle morphology on the competing interplay between heating and pyrolysis processes. In addition, the Lagrangian method cannot be applied to model pyrolysis of plastic particles with diameters larger than 2 mm. These aspects should be taken into account when modeling a large number of plastic particles by means of the Lagrangian approach due to the assumption of homogeneity. The correlation of pyrolysis time vs. pyrolysis number can serve as a first-order estimate for assessing the required residence time at given heating conditions.

Acknowledgements The authors gratefully acknowledge the financial support by the Helmholtz Association of German Research Centers (HGF), within the research program MTET (Materials and Technologies for the Energy Transition). This work utilized computing resources from the Horeka and the bwUniCluster-2 clusters at the Steinbuch Centre for Computing (SCC) at the Karlsruhe Institute of Technology in Germany.

Author Contributions F. Z.: designed research, performed research, wrote the paper S.T.: designed research, supervised the work, revised the paper F.G.: developed the code, revised the paper D.S.: designed research, acquisition of funding, reviewed the manuscript.

Funding Open Access funding enabled and organized by Projekt DEAL.

Data Availability No datasets were generated or analysed during the current study.

Declarations

Competing interests The authors declare no competing interests.

References

1. Geyer R, Jambeck JR, Law KL (2017) Production, use, and fate of all plastics ever made. Sci Adv 3:1700782. https://doi.org/10.1126/sciadv.1700782
2. Tokmurzin D, Nam JY, Lee TR, Park SJ, Nam H, Yoon SJ, Mun TY, Yoon SM, Moon JH, Lee JG, Lee DH, Ra HW, Seo MW (2022) High temperature flash pyrolysis characteristics of waste plastics (SRF) in a bubbling fluidized bed: Effect of temperature and pelletizing. Fuel 326. https://doi.org/10.1016/j.fuel.2022.125022
3. Sharuddin SDA, Abnisa F, Daud W, Aroua MK (2016) A review on pyrolysis of plastic wastes. Energy Convers Manage 115:308–326. https://doi.org/10.1016/j.enconman.2016.02.037
4. Bockhorn H, Hornung A, Hornung U (1999) Mechanisms and kinetics of thermal decomposition of plastics from isothermal and dynamic measurements. J Anal Appl Pyrolysis 50(2):77–101. https://doi.org/10.1016/S0165-2370(99)00026-1
5. Gascoin N, Navarro-Rodriguez A, Gillard P, Mangeot A (2012) Kinetic modelling of high density polyethylene pyrolysis: Part 1. comparison of existing models. Polym Degrad Stab 97:1466–1474. https://doi.org/10.1016/j.polymdegradstab.2012.05.008

6. Schubert T, Lechleitner A, Lehner M, Hofer W (2020) 4-lump kinetic model of the co-pyrolysis of ldpe and a heavy petroleum fraction. Fuel 262. https://doi.org/10.1016/j.fuel.2019.116597
7. Locaspi A, Pelucchi M, Faravelli T (2023) Towards a lumped approach for solid plastic waste gasification: Polystyrene pyrolysis. J Anal Appl Pyrolysis 171. https://doi.org/10.1016/j.jaap.2023.105960
8. Kusenberg M, Eschenbacher A, Djokic MR, Zayoud A, Ragaert K, De Meester S, Van Geem KM (2022) Opportunities and challenges for the application of post-consumer plastic waste pyrolysis oils as steam cracker feedstocks: To decontaminate or not to decontaminate? Waste Manage 138:83–115. https://doi.org/10.1016/j.wasman.2021.11.009
9. Armenise S, SyieLuing W, Ramírez-Velásquez JM, Launay F, Wuebben D, Ngadi N, Rams J, Muñoz M (2021) Plastic waste recycling via pyrolysis: A bibliometric survey and literature review. J Anal Appl Pyrolysis 158. https://doi.org/10.1016/j.jaap.2021.105265
10. López A, De Marco I, Caballero B, Laresgoiti M, Adrados A (2011) Influence of time and temperature on pyrolysis of plastic wastes in a semi-batch reactor. Chem Eng J 173(1):62–71. https://doi.org/10.1016/j.cej.2011.07.037
11. Zeller M, Netsch N, Richter F, Leibold H, Stapf D (2021) Chemical recycling of mixed plastic wastes by pyrolysis-pilot scale investigations. Chem Ing Tech 93(11):1763–1770. https://doi.org/10.1002/cite.202100102
12. Rajendran KM, Chintala V, Sharma A, Pal S, Pandey JK, Ghodke P (2020) Review of catalyst materials in achieving the liquid hydrocarbon fuels from municipal mixed plastic waste (MMPW). Mater Today Commun 24. https://doi.org/10.1016/j.mtcomm.2020.100982
13. Ratnasari DK, Nahil MA, Williams PT (2017) Catalytic pyrolysis of waste plastics using staged catalysis for production of gasoline range hydrocarbon oils. J Anal Appl Pyrolysis 124:631–637. https://doi.org/10.1016/j.jaap.2016.12.027
14. Miskolczi N, Juzsakova T, Sója J (2019) Preparation and application of metal loaded zsm-5 and y-zeolite catalysts for thermocatalytic pyrolysis of real end of life vehicle plastics waste. J Energy Inst 92:118–127. https://doi.org/10.1016/j.joei.2017.10.017
15. Munir D, Amer H, Aslam R, Bououdina M, Usman MR (2020) Composite zeolite beta catalysts for catalytic hydrocracking of plastic waste to liquid fuels. Mater Renew Sustain Energy 9. https://doi.org/10.1007/s40243-020-00169-3
16. Gopinath S, Devan PK, Pitchandi K (2020) Production of pyrolytic oil from uldp plastics using silica-alumina catalyst and used as fuel for di diesel engine. RSC Adv 10:37266–37279. https://doi.org/10.1039/d0ra07073d
17. Jung SH, Cho MH, Kang BS, Kim JS (2010) Pyrolysis of a fraction of waste polypropylene and polyethylene for the recovery of BTX aromatics using a fluidized bed reactor. Fuel Process Technol 91:277–284. https://doi.org/10.1016/j.fuproc.2009.10.009
18. Kaminsky W (2021) Chemical recycling of plastics by fluidized bed pyrolysis. Fuel Commun 8:100023. https://doi.org/10.1016/j.jfueco.2021.100023
19. Liu F, Li C, Zeng X, Chen J, Guan J, Yang L (2024) Study on the flow and collision characteristics of catalyst particles in fcc reactor. Powder Technol 438:119642. https://doi.org/10.1016/j.powtec.2024.119642
20. Zhao Y, Shi X, Wang C, Lan X, Gao J (2023) Study on flow characteristics of turbulent fluidized bed with variable gas velocity due to chemical reactions. Powder Technol 416:118211. https://doi.org/10.1016/j.powtec.2022.118211
21. Zhao Y, Shi X, Lan X, Gao J, Jing W, Xiong Q (2024) Simulation analysis of micro-explosion during emulsification feeding of residue fluidized catalytic cracking. Appl Therm Eng 250:123514. https://doi.org/10.1016/j.applthermaleng.2024.123514
22. Shi X, Liu H, Zhang X, Lan X, Gao J (2023) Numerical simulation on effects of biomass type on its fast pyrolysis in fluidized bed reactor. Indust Eng Chem Res 62(42):17100–17108. https://doi.org/10.1021/acs.iecr.3c01454
23. Alobaid F, Almohammed N, Farid MM, May J, Rößger P, Richter A, Epple B (2022) Progress in CFD simulations of fluidized beds for chemical and energy process engineering. Prog Energy Combust Sci 91:109930. https://doi.org/10.1016/j.pecs.2021.100930
24. Zhang F, Tavakkol S, Dercho S, Zhou J, Zirwes T, Zeller M, Vogt J, Zhang R, Bockhorn H, Stapf D (2024) Assessment of dynamic characteristics of fluidized beds via numerical simulations. Phys Fluids 36(2):023348. https://doi.org/10.1063/5.0189519
25. Mazloum S, Awad S, Allam N, Aboumsallem Y, Loubar K, Tazerout M (2021) Modelling plastic heating and melting in a semi-batch pyrolysis reactor. Appl Energy 283:116375. https://doi.org/10.1016/j.apenergy.2020.116375
26. Lopez G, Artetxe M, Amutio M, Bilbao J, Olazar M (2017) Thermochemical routes for the valorization of waste polyolefinic plastics to produce fuels and chemicals. a review. Renew Sustain Energy Rev 73:346–368. https://doi.org/10.1016/j.rser.2017.01.142
27. Dogu O, Pelucchi M, Vijver RV, Steenberge PHMV, D'hooge DR, Cuoci A, Mehl M, Frassoldati A, Faravelli T, Geem KMV (2021) The chemistry of chemical recycling of solid plastic waste via pyrolysis and gasification: State-of-the-art, challenges, and future directions. Prog Energy Combust Sci 84. https://doi.org/10.1016/j.pecs.2020.100901
28. Armenise S, Wong S, Ramírez-Velásquez JM, Launay F, Wuebben D, Nyakuma BB, Rams J, Muñoz M (2021) Application of computational approach in plastic pyrolysis kinetic modelling: a review. React Kinet Mech Catal 134(2):591–614. https://doi.org/10.1007/s11144-021-02093-7
29. Yin F, Zhuang Q, Chang T, Zhang C, Sun H, Sun Q, Wang C, Li L (2021) Study on pyrolysis characteristics and kinetics of mixed plastic waste. J Mater Cycles Waste Manag 23(5):1984–1994. https://doi.org/10.1007/s10163-021-01271-y
30. Das P (2024) Pyrolysis study of a waste plastic mixture through different kinetic models using isothermal and nonisothermal mechanism. RSC Adv 14(35):25599–25618. https://doi.org/10.1039/d4ra04957h
31. Netsch N, Schröder L, Zeller M, Neugber I, Merz D, Klein CO, Tavakkol S, Stapf D (2024) Thermogravimetric study on thermal degradation kinetics and polymer interactions in mixed thermoplastics. J Therm Anal Calorim. https://doi.org/10.1007/s10973-024-13630-6
32. Zhang F, Cao J, Zirwes T, Netsch N, Tavakkol S, Zhang R, Bockhorn H, Stapf D (2024) Numerical Simulation of Thermal Decomposition of Polyethylene with a Single-Particle Model. Springer, pp 180–191. https://doi.org/10.1007/978-3-031-67241-5_17
33. Ding K, Xiong Q, Zhong Z, Zhong D, Zhang Y (2020) Cfd simulation of combustible solid waste pyrolysis in a fluidized bed reactor. Powder Technol 362:177–187. https://doi.org/10.1016/j.powtec.2019.12.011
34. Zhang M, Zhang Y, Ma D, Li A, Fu W, Ji G, Dong J (2022) Numerical investigation on the heat transfer of plastic waste pyrolysis in a rotary furnace. Chem Eng J 445:136686. https://doi.org/10.1016/j.cej.2022.136686
35. Attanayake D, Sewerin F, Kulkarni S, Dernbecher A, Alonso AD, Wachem B (2023) Review of modelling of pyrolysis processes with CFD-DEM. Flow Turbul Combust 111:355–408. https://doi.org/10.1007/s10494-023-00436-z
36. Ceamanos J, Mastral J, Millera A, Aldea M (2002) Kinetics of pyrolysis of high density polyethylene comparison of isothermal and dynamic experiments. J Anal Appl Pyrolysis 65(2):93–110. https://doi.org/10.1016/S0165-2370(01)00183-8

37. Areeprasert C, Asingsamanunt J, Srisawat S, Kaharn J, Inseemeesak B, Phasee P, Khaobang C, Siwakosit W, Chiemchaisri C (2017) Municipal plastic waste composition study at transfer station of bangkok and possibility of its energy recovery by pyrolysis. Energy Procedia 107:222–226. https://doi.org/10.1016/j.egypro.2016.12.132
38. Netsch N, Zeller M, Richter F, Bergfeldt B, Tavakkol S, Stapf D (2024) Energy demand for pyrolysis of mixed thermoplastics and waste plastics in chemical recycling: Model prediction and pilot-scale validation. ACS Sustain Resourc Manag 1(7):1485–1492. https://doi.org/10.1021/acssusresmgt.4c00109
39. Kabelac S, Kind M, Mewes H, Schaber K, Stephan P (2013) VDI-Wärmeatlas, 11th edn. Springer, Berlin, Heidelberg. https://link.springer.com/referencework/10.1007/978-3-642-19981-3
40. Żuk PJ, Tużnik B, Rymarz T, Kwiatkowski K, Dudyński M, Galeazzo FCC, Filho GCK (2022) Openfoam solver for thermal and chemical conversion in porous media. Comput Phys Commun 278. https://doi.org/10.1016/j.cpc.2022.108407
41. Ruiz MP, Zairin DM, Kersten SR (2023) On the intrinsic reaction rate of polyethylene pyrolysis and its interplay with mass transfer. Chem Eng J 469:143886. https://doi.org/10.1016/j.cej.2023.143886